

# A review of covalent organic framework electrode materials for rechargeable metal-ion batteries

ZENG Shu-mao<sup>1,2,†</sup>, HUANG Xiao-xiong<sup>1,2,†</sup>, MA Ying-jie<sup>1,\*</sup>, ZHI Lin-jie<sup>1,2,\*</sup>

(1. CAS Key Laboratory of Nanosystem and Hierarchical Fabrication, CAS Center for Excellence in Nanoscience,

National Center for Nanoscience and Technology, Beijing 100190, China;

2. University of Chinese Academy of Sciences, Beijing 100049, China )

**Abstract:** Covalent organic frameworks (COFs) are highly promising electrode materials for next-generation rechargeable metal-ion batteries owing to their robust framework, abundant electrochemically active sites, well-defined and tunable pores and channels for metal ion transfer, and adjustable molecular structures for improving electrochemical performance. Moreover, COFs do not have the problems caused by expensive or toxic elements in conventional inorganic electrode materials or the cycling stability challenges existing in small organic molecules, and thus have great potential as electrode materials in next-generation rechargeable metal-ion batteries. We summarize the electrochemically active sites of these materials for charge storage, and most importantly, we focus on strategies for improving their electrochemical performance, including energy density, rate performance and cycling life by changing their frameworks, pores, active sites, and electronic structures. To fabricate high performance COF electrodes, much more effort is needed to improve their ionic and electronic conductivities, increase their operating voltage, and reveal their mechanisms of energy storage. This review may shed light on developing high performance COF electrode materials for next-generation rechargeable metal-ion batteries.

**Key words:** Covalent organic frameworks; Rechargeable metal-ion batteries; Energy density; Rate performance; Cyclic lifespan

## 1 Introduction

Due to the aggressive consumption of fossil fuels and ever-increasing energy demands as well as adverse greenhouse effect, the efficient utilization of renewable power sources (e.g., wind, solar, and tidal energy), which cannot be used directly, has become the most significant issue that must be confronted with<sup>[1-3]</sup>. Electrochemical energy storage systems are considered as the key technology for the development of intermittent energy resources<sup>[4]</sup>. As one of the main sustainable energy-storage technologies, rechargeable metal-ion batteries (RMBs: Li, Na, Mg, K, Ca, Zn, Al, etc.)<sup>[5-11]</sup>, are gaining much more attentions because they meet the demands of green energy with high energy density, cleanliness and high efficiency. Notably, the electrochemical performance of metal-ion batteries depends on the electrode materials, including inorganic and organic materials. For instance, lithium-ion batteries (LIBs), since it was first commercialized by Sony Co. in 1991<sup>[12, 13]</sup>, employ ion-inser-

tion materials such as  $\text{LiCoO}_2$ <sup>[14]</sup>,  $\text{LiMn}_2\text{O}_4$ <sup>[15]</sup>, and  $\text{LiFePO}_4$ <sup>[16]</sup>, as the cathode materials and graphite<sup>[17, 18]</sup> or even silicon<sup>[19-21]</sup> as the anode materials. However, LIBs are hard-pressed to meet the growing demands, such as low cost, high safety, high energy density and long cycling stability. Despite the rapid development of RMBs, they are primarily based on inorganic electrode materials such as transitional metal oxides and graphite, which are reaching their capacity limitation. In addition, the limited natural resources and environmental issues have yet hindered RMBs to achieve widespread applications<sup>[22, 23]</sup>.

As an indispensable application in grid electrical energy storage<sup>[24]</sup>, RMBs need to meet the demand of high energy density, namely, a large specific capacity, a high voltage and low weight. When it comes to the electrical vehicles and consumer electronics, in addition to a prominent energy density, an outstanding rate performance is also essential for the RMBs<sup>[25, 26]</sup> to meet the power demand for various kinds of applica-

**Received date:** 2021-01-11; **Revised date:** 2021-01-13

**Corresponding author:** MA Ying-jie, Assistant researcher. E-mail: [mayj@nanoctr.cn](mailto:mayj@nanoctr.cn);

ZHI Lin-jie, Professor. E-mail: [zhilj@nanoctr.cn](mailto:zhilj@nanoctr.cn)

**Author introduction:** †These authors contributed equally to this work.

tions. Besides, the excellent cycling performance is quite vital as well, since considering economic cost, the RMBs should possess a service life as long as possible no matter where they are used<sup>[27]</sup>. However, the performance of RMBs is limited by current technology, especially materials. Therefore, developing novel materials for all components (i.e. anode, cathode, separator and electrolyte) with high performance is of vital importance to enhance the energy density, rate performance and cycling stability of RMBs<sup>[28–30]</sup>.

Recently, microporous organic polymers have been widely used in the fields of catalysis<sup>[31–35]</sup>, separation<sup>[36–38]</sup>, drug delivery<sup>[39, 40]</sup>, gas absorption and water storage<sup>[41, 42]</sup>, owing to their robust networks, open channels and structural stability<sup>[43]</sup>. Since the groundbreaking work by Yaghi and co-workers in the 2005<sup>[44]</sup>, the chemical synthesis of covalent organic frameworks (COFs) have progressed significantly as they show great potential for functional exploration. As a new kind of crystalline porous materials, COFs are a class of fully pre-designable polymers with atomically precise integration of building blocks into a two-(2D) or three-(3D)-dimensional topologies characterized by light-weight elements (C, H, O, and N) and strong covalent bonds, which enables the integration of organic units into well-defined primary- and high-order structures. Meanwhile, not only their skeletons are designed, but also their pore size, shape, interface, and environment can be predetermined via either polycondensation or post-synthetic functionalization. Therefore, those features endow COFs unique conformations and morphologies that generate confined molecular space and interface to interplay with photons, electrons, holes, spins, ions, and molecules<sup>[45–49]</sup>.

In RMBs, anchoring redox-active units on COF skeletons by covalent bonds is expected to boost the electrochemical performance by introducing plenty of electrochemical active sites. Additionally, the open channels of COFs can also accelerate ion transport, which is necessary for the high-rate performance<sup>[50]</sup>. Most importantly, their electrochemical performance in RMBs can be improved through tuning their microstructures<sup>[51]</sup>. Therefore, COFs have attracted consid-

erable research interests in energy storage, and remarkable efforts have been devoted to designing and synthesizing advanced COFs.

In this review, we have summarized electrochemically active sites of COFs for charge storage and illustrated the strategies for improving their electrochemical performance in RMBs, including energy density, rate performance and cyclic lifespan through tuning their frameworks, pores, active sites and electronic structures. In the last section, we summarize the challenges in COF electrode materials and give possible solutions.

## 2 Electrochemical active sites in COFs

COF electrode materials bear plenty of electrochemically active sites, which are redox units and can bind positive/negative charges through redox states during charging/discharging process to realize energy storage. To fabricate RMBs with high energy density, COF electrode materials in RMBs usually are given carbonyl (amides and quinones), imine, and conjugated heterocycles as the active sites (Fig. 1). These redox groups are assigned to n-type organics, the redox processes of which take place between the neutral state and the charged state—for p-type organics, the redox processes occur between the neutral state and the positively charged state.

In RMBs, n-type organics, such as naphthalene dianhydride (Fig. 1a) and quinones (Fig. 1b, c, and k), are firstly be reduced and combine with metal counterions such as  $\text{Li}^+$ ,  $\text{Na}^+$  or  $\text{Mg}^{2+}$  (Fig. 1). COFs with n-type organics can serve not only as anode materials but also cathode materials, which depends on their structure and redox potentials (versus  $\text{Li}^{+/0}$ ). For instance, COFs bearing redox groups with low redox potentials ( $< 1.6 \text{ V}$  versus  $\text{Li}^{+/0}$ ), such as naphthalene dianhydride (Fig. 1a), work as anode materials, which should be coupled with high-voltage cathode materials such as  $\text{LiCoO}_2$  to fabricate a full LIB. This LIB needs to be charged firstly, during which carbonyls in naphthalene dianhydride groups are reduced to enolates and bind  $\text{Li}^+$  from the electrolyte, and  $\text{LiCoO}_2$  is oxidized and releases  $\text{Li}^+$  into the electrolyte.

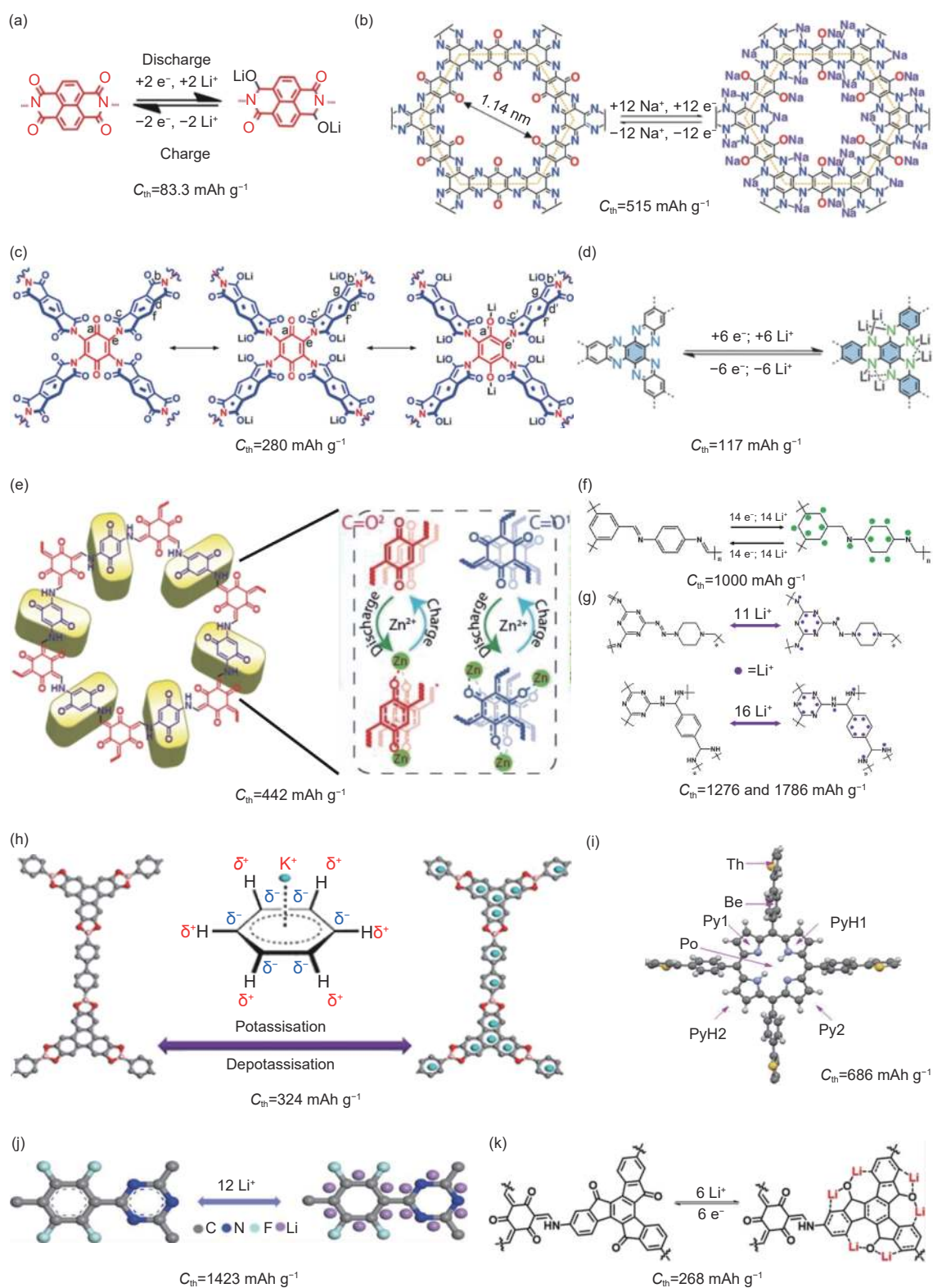


Fig. 1 Various electrochemical active sites in reported COFs and corresponding theoretical specific capacity ( $C_{th}$ )<sup>[52-62]</sup>. (a, b, f) reproduced by permission of Nature Publishing Group, (c, d, g, k) reproduced by permission of Wiley-VCH, (e) reproduced by permission of the Royal Society of Chemistry and (h, i, j) reproduced by permission of American Chemical Society.

In contrast, COFs based on carbonyl group existing in five- or six-member carbon circle (Fig. 1b, c, e, and k) and groups that can undergo over lithiation and

potassiation (Fig. 1d, f, h and j), often exhibit a high distinct reduction potential (2-3 V versus  $Li^{+/0}$ ), and thus usually work as cathode materials. Notably, these

COF cathode materials do not initially contain Li, and consequently should be coupled with a Li-containing anode material such as lithium metal to afford a battery. When this battery starts to work, it will be discharged, and the COF cathode materials will be reduced.

It should be noted that the number of carbonyl group cannot determine the specific capacity of COF electrodes in a direct way. As shown in Fig. 1a, 4 carbonyl groups in a unit only bond with 2 Li<sup>+</sup>, but 3 carbonyl groups can bond with 6 Li<sup>+</sup> (Fig. 1k), leading to a higher utilization of carbonyl groups. Apparently, it can be concluded that the chemical environment of the local molecular structure and space steric hindrance determine the utilization of active sites as well. As a result, the specific capacity of COF electrode materials relies on not only the number of active sites but also the local molecular structure and stereochemical structure, which should be considered when new COF electrode materials are designed.

Additionally, the imine groups (or C=N double bond) are also a vital kind of active sites in COFs, which are usually generated from Schiff-base reaction (Fig. 1f and g), triazine cyclization reaction (Fig. 1j) or triple condensation reaction between carbonyl group and amidogen group (Fig. 1b and d). Moreover, special attention should be paid to the aromatic rings in COF electrode materials, which feature unique electrochemical activities. It has been reported that the aromatic rings in COF electrode materials can bond with metal ions and work as active sites (as shown in Fig. 1f-j) under some special conditions, for instance, when they are hybridized with carbon nanotube (CNT)<sup>[57-59]</sup>, or bonded with fluorine atom<sup>[61]</sup>, leading to the reversibility of the exhaustive-lithiation (referred to as ‘overlithiation’) process or positively charged aromatic rings. However, there are other studies holding the view that the aromatic ring is electrochemically inactive<sup>[63]</sup> or demonstrate no capacity<sup>[64, 65]</sup>. Evidently, much effort should be devoted to exploring the mechanism of COF electrode materials in RMBs in the future.

### 3 Tunable electrochemical performance of COFs in RMBs’ application

Featuring large amount of light-weight component atoms, tunable molecular structure and eminent thermal and chemical stability, COFs are highly promising electrode materials for RMBs. Most importantly, because of the tunable structures, the electrochemical performance of COF electrode materials, including energy density, rate performance and cyclic lifespan, can be improved by adjusting their structures. The performance of typical COF electrode materials in RMBs are summarized in Table 1.

#### 3.1 Energy density

Long battery life is critical to electronic devices and electrical vehicles, which is determined by energy density of RMBs. The energy density of RMBs can be enhanced by optimizing electrode materials, electrolytes, and architectures of RMBs. For electrode materials, the energy density can be improved by increasing the specific capacity and working voltage of electrode materials, which can be achieved more easily by COF electrode materials compared to conventional inorganic electrode materials because of the unique features of COFs.

The specific capacity of electrodes is determined by the number of electrons exchanged between them and the external circuit during charging/discharging process and the molar mass of the material. COFs often offer many active sites with light-weight atoms in the primitive unit cell (Fig. 1), which render COFs an ultrahigh specific capacity compared with inorganic materials<sup>[90-93]</sup>. Notably, to realize COF electrodes with high energy density, the utilization of active sites in COFs needs to be maximized although COFs have high theoretical specific capacity. In other words, the active sites in COFs should be exposed as many as possible, and thus they are accessible by the ions from electrolyte and can get electrons from the external circuit. For instance, Wang et al.<sup>[57]</sup> synthesized a COF based on the Schiff-base reaction between aromatic-1,3,5-trialdehyde and 1,4-phenylenediamine which was hybridized with carbon nanotubes (CNTs). The composite electrode shows a current peak (at around



**Table 1 The representative COF electrode materials in RBMs.**

| COFs' name                    | Application Scenarios | Current density (mA g <sup>-1</sup> )/<br>Specific capacity (mAh g <sup>-1</sup> ) | Voltage Window (V) | Lifespan (cycles)/<br>Capacity retention (%) | Current density (A g <sup>-1</sup> )/<br>Specific capacity (mAh g <sup>-1</sup> ) | Ref. |
|-------------------------------|-----------------------|--|--------------------|--|---|------|
| DTP-ANDI-COF@CNT              | LIB                   | 200/70   | 1.5-3.5            | 700/100                                      | 1/60  | [52] |
| PIBN-COF@Graphene             | LIB                   | 28/271   | 1.5-3.5            | 300/86                                       | 2.8/200   | [54] |
| DAAQ-TFP-COF                  | LIB                   | 20/110   | 1.5-4              | 1000/100                                     | 3/20  | [66] |
| DAAQ-ECOF                     | LIB                   | 20/145   | 1.5-4              | 1800/100                                     | 3/50  | [66] |
| DAAQ-COF                      | SIB                   | 100/420  | 0.05-3             | 10000/99                                     | 5/200   | [67] |
| DABQ-ECOF                     | LIB                   | 20/ ~ 200  | 1.5-3.5            | /  | /   | [66] |
| TEMPO-ECOF                    | LIB                   | 20/ ~ 100  | 2-4                | /  | /   | [66] |
| TQBQ-COF                      | SIB                   | 20/350   | 1-3.6              | 1000/96                                      | 10/134  | [53] |
| TRO-COF                       | LIB                   | 27.4/268   | 0.5-4.5            | 100/99.9                                     | 0.548/100   | [62] |
| N <sub>2</sub> -COF           | LIB                   | 1000/700   | 0.05-3             | 500/75                                       | 5/500   | [68] |
| N <sub>3</sub> -COF           | LIB                   | 1000/700   | 0.05-3             | 500/65                                       | 5/550   | [68] |
| Tp-DANT-COF                   | LIB                   | 200/78.9   | 1.5-4              | 600/90                                       | 2/70  | [64] |
| Tb-DANT-COF                   | LIB                   | 50/135   | 1.5-4              | 300/83                                       | 2/67  | [64] |
| rCTF                          | LIB                   | 300/1190   | 0.005-3            | 1500/100                                     | 12/500  | [69] |
| PI-ECOF-1                     | LIB                   | 14.2/112   | 1.5-3.5            | 300/75                                       | 0.284/70  | [65] |
| PI-ECOF-2                     | LIB                   | 12.8/103   | 1.5-3.5            | 300/75                                       | 0.256/40  | [65] |
| TFPB-TAPT COF                 | SIB                   | 30/200   | 0.05-1.6           | 500/50.8                                     | 0.2/145   | [70] |
| BQ1-COF                       | LIB                   | 39/502   | 1.2-3.5            | 1000/81                                      | 7.73/171  | [71] |
| C <sub>2</sub> N-450          | LIB                   | 37.2/933   | 0.02-3             | 500/130.6                                    | 3.72/40.1   | [72] |
| C <sub>3</sub> N              | LIB                   | 37.2/787   | 0.02-3             | 500/91                                       | 3.72/180  | [72] |
| PGF-1                         | LIB                   | 500/480  | 1-3.5              | 1400/78.3                                    | 5/200   | [73] |
| DBA-COF 3                     | LIB                   | 50/200   | 0.05-3             | 90/100                                       | 1/90  | [74] |
| AQ-COF@CNT                    | LIB                   | 50/71  | 1.5-3.5            | 3000/100                                     | 2.5/11  | [75] |
| TThPP                         | LIB                   | 1000/400   | 0.005-3            | 200/100                                      | 4/200   | [60] |
| JUC-526                       | LIB                   | 200/441.2  | 0.01-3             | 500/100                                      | 2/200   | [76] |
| HATN-CMP                      | LIB                   | 100/150  | 1.5-4              | 50/60  | 1/50  | [77] |
| IISERP-CON1                   | LIB                   | 100/720  | 0.01-3             | 1000/100                                     | 2/460   | [78] |
| IISERP-COF16                  | SIB                   | 100/80   | 0.01-3             | 500/100                                      | /   | [79] |
| IISERP-COF17                  | SIB                   | 100/200  | 0.01-3             | 500/100                                      | 1/100   | [79] |
| IISERP-COF18                  | SIB                   | 100/400  | 0.01-3             | 1400/92                                      | 15/127  | [79] |
| Pa-COF                        | LIB                   | 1000/401.3   | 0.01-3.5           | 2000/74.8                                    | 5/141.8   | [80] |
| Tb-COF                        | LIB                   | 1000/379.1   | 0.01-3.5           | 2000/72.7                                    | 5/144   | [80] |
| TAPB-terephthal Aldehyde COFs | SIB                   | 100/303  | 0-3                | 1000/85                                      | 5/150   | [81] |
| Cz-COF1                       | LIB                   | 200/300  | 0.01-3             | 400/59                                       | 1/200   | [82] |
| Cz-COF2                       | LIB                   | 200/250  | 0.01-3             | 400/50                                       | 1/100   | [82] |
| Tp-Azo-COF                    | LIB                   | 1000/306   | 0.01-3             | 3000/100                                     | 2.4/100   | [83] |
| TpBpy                         | AIB                   | 2000/150   | 0.01-2.3           | 13000/100                                    | 5/113   | [84] |
| CTF-0                         | KIB                   | 100/100  | 0.01-3             | 350/67                                       | 1/63  | [85] |
| CTF-1                         | KIB                   | 100/50   | 0.01-3             | 350/67                                       | 1/31  | [85] |
| DAPT-TFP-CPF                  | SIB                   | 100/150  | 0.8-3.2            | 1400/94.7                                    | 5/100   | [86] |
| PDI-Tc                        | LIB                   | 190/45   | 1.8-3.2            | 500/80                                       | 0.482/22  | [87] |
| HqTp-COF                      | ZIB                   | 625/150  | 0.2-1.8            | 1000/95                                      | 1.25/125  | [56] |
| COF-CNT                       | LIB                   | 100/1536   | 0.005-3            | 500/510                                      | 5/200   | [54] |
| 2D CCP-HATN                   | LIB                   | 500/116  | 1.2-3.9            | 1000/91                                      | 1/94  | [55] |
| E-CIN-1/CNT                   | LIB                   | 100/538  | 0.001-3            | 250/124                                      | 5/97  | [58] |
| E-SNW-1/CNT                   | LIB                   | 100/542  | 0.001-3            | 250/91                                       | 5/212   | [58] |
| COF-10@CNT                    | KIB                   | 100/288  | 0.005-3            | 4000/54                                      | 5/68  | [59] |
| E-TFPB-COF/MnO <sub>2</sub>   | LIB                   | 100/1250   | 0.005-3            | 300/135                                      | 5/500   | [88] |
| Si@COF                        | LIB                   | 1000/2000  | 0.01-1             | 1000/60                                      | 5/1000  | [89] |

1.5 V) corresponding to lithiation of imine units (C=N) in the cyclic voltammetry (CV) curve, and reduction current peaks of aromatic ring at ~ 0.72, 0.12

and 0.06 V (Fig. 2d), meaning that there are several kinds of active groups that undergo redox processes during charging/discharging process. Therefore, the

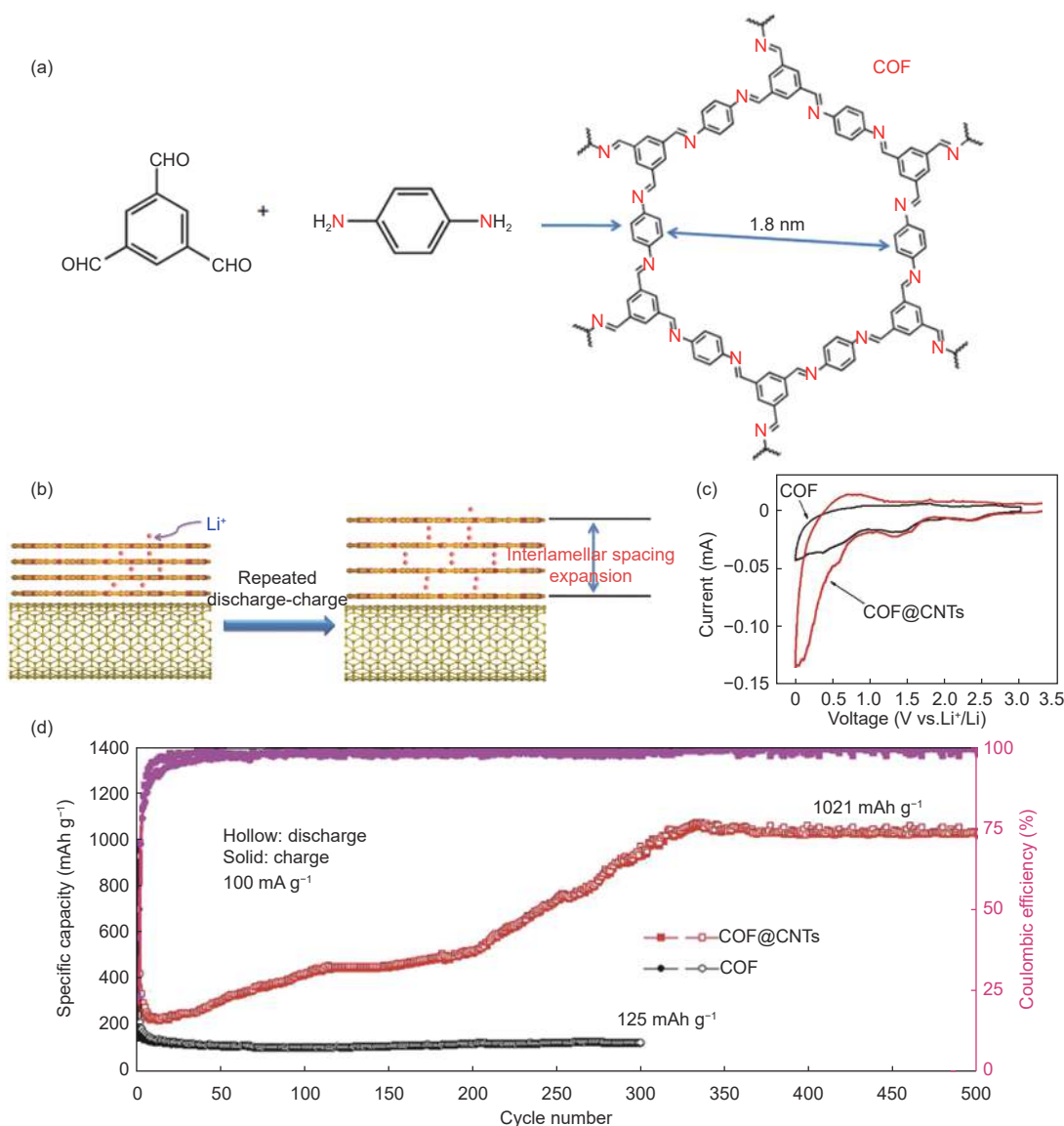


Fig. 2 The composite COF@CNT electrode<sup>[57]</sup>: (a) structure of the COF, (b) interlayer spacing expansion, (c) the cyclic voltammetry curves and (d) the electrochemical performance of the composite electrode (Reproduced by permission of Nature Publishing Group).

COF@CNT electrode displays an ultrahigh specific capacity of  $1\,021\text{ mAh g}^{-1}$  at  $100\text{ mA g}^{-1}$ , but the pure COF only shows a limited capacity of  $125\text{ mAh g}^{-1}$  at the same current density. The big difference in the specific capacities of COF@CNT and pure COF should come from the different numbers of exposed active sites. After it is hybridized with CNTs, the interlayer space in the COF is expanded gradually (Fig. 2b) during the charge-discharge cycles, which facilitates transfer of ions to the aromatic rings, meaning that more active sites and aromatic rings become accessible by ions. In addition, the conductivity of COF electrodes is improved by hybridizing COF elec-

trode materials with CNTs in the meantime.

Besides exposing the active sites, high specific capacity can be realized by incorporating more active sites into the repeating units of COFs. In 2020 Rodney S. Ruoff et al.<sup>[69]</sup> built a covalent triazine framework (CTF) composed of triazine rings and anthraquinone groups by the reaction between 2,6-diformyl-9,10-anthraquinone and terephthalamidine dihydrochloride (Fig. 3a), which showed an excellent charge storage capacity of  $1\,190\text{ mAh g}^{-1}$  at the current density of  $300\text{ mA g}^{-1}$  (Fig. 3b). Theoretical analysis of the molecular structure and the lithiation process of the CTF by density functional theory (DFT) together with

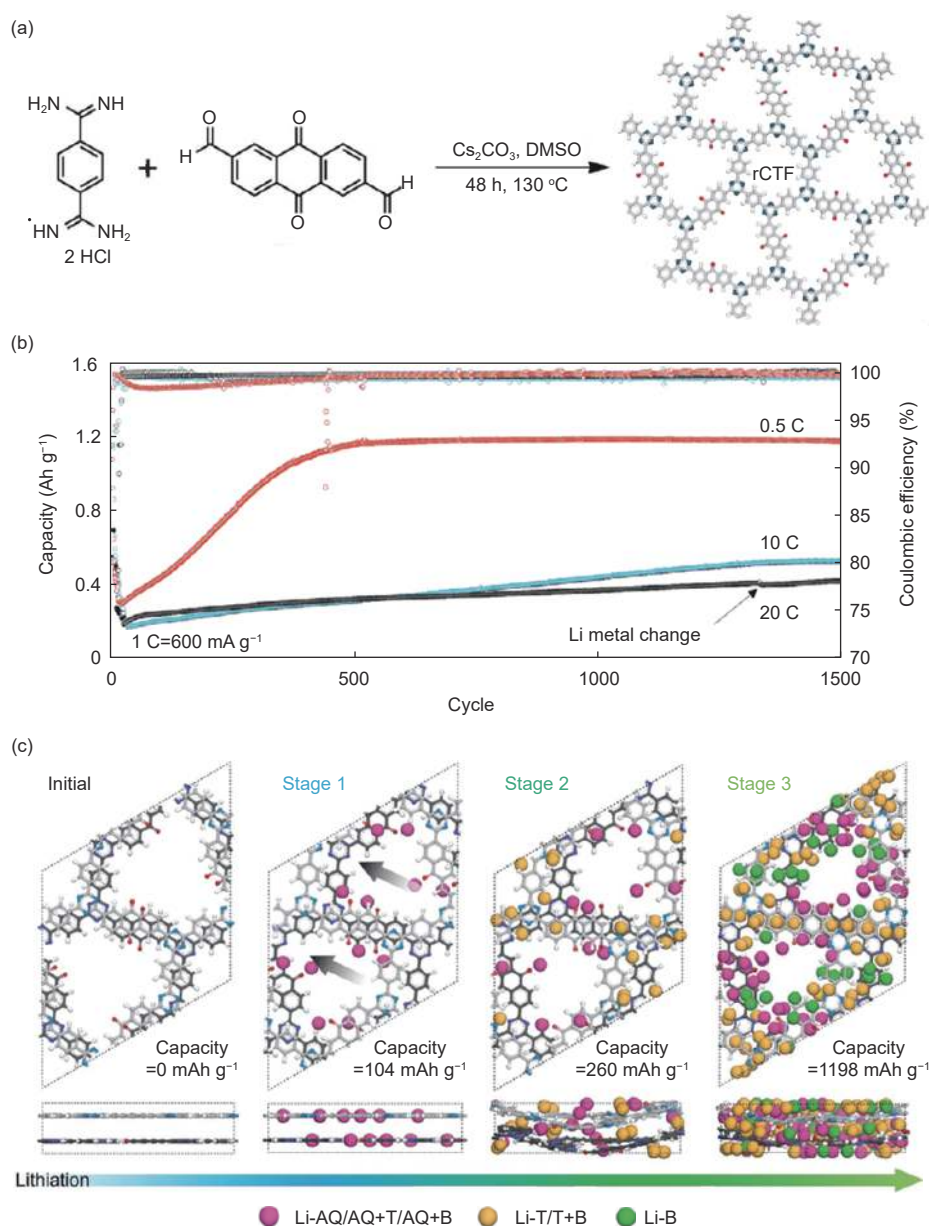


Fig. 3 (a) The structure and synthetic method for rCTF, (b) the electrochemical performance of rCTF and (c) the simulated lithium storage mechanism<sup>[69]</sup> (Reproduced by permission of Wiley-VCH).

Monte Carlo (MC) simulation shows that anthraquinone groups, triazine rings and aromatic rings undergo lithiation reactions orderly as the active sites and are exposed increasingly, involving a 23-electron process in the lithiation/delithiation process and thus leading to high specific capacity.

And the utilization efficiency of active sites in COFs can be improved by exfoliating stacked COFs into few-layer nanosheets<sup>[88]</sup>. TFPB-COF was prepared by condensation of PPDA and TFPB (Fig. 4a) followed by exfoliation via a chemical method, which

displays a capacity as high as  $968\text{ mAh g}^{-1}$  after 300 cycles at  $100\text{ mA g}^{-1}$ . In addition, the composite of E-TFPB-COF and  $\text{MnO}_2$ , E-TFPB-COF/ $\text{MnO}_2$ , delivers a higher specific capacity of  $1359\text{ mAh g}^{-1}$  after 300 cycles at  $100\text{ mA g}^{-1}$ . In the composite,  $\text{MnO}_2$  nanoparticles act as the "spacer" to effectively prevent the agglomeration of E-TFPB-COF during cycling, further improving the performance of E-TFPB-COF.

Another approach to achieve higher energy density is to enhance the working voltage of the RMBs (cathode versus anode), which is strongly associated

with the redox potential (versus  $\text{Li}^{+/0}$ ) of active sites in COFs, and thus can be improved by molecular engineering (Fig. 5)<sup>[97]</sup>.

It has been reported that the working potential (versus  $\text{Li}^{+/0}$ ) of organic electrodes can be tuned by adjusting their lowest unoccupied molecular orbital

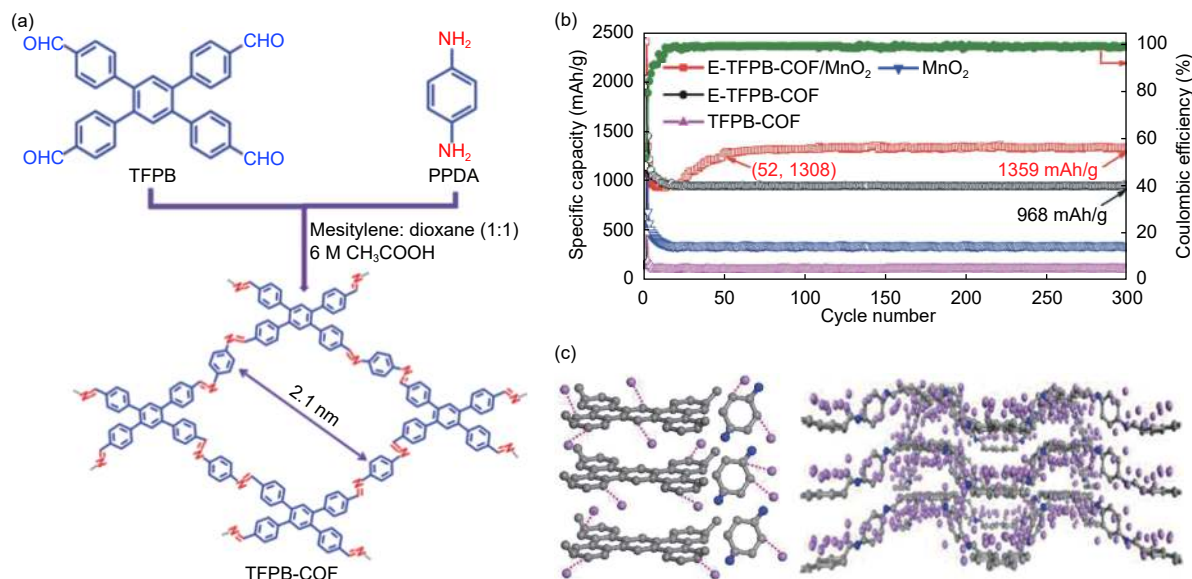


Fig. 4 (a) The synthetic route of TFPB-COF, (b) the electrochemical performance of TFPB-COF and (c) the lithium storage mechanism<sup>[88]</sup> (Reproduced by permission of Wiley-VCH).

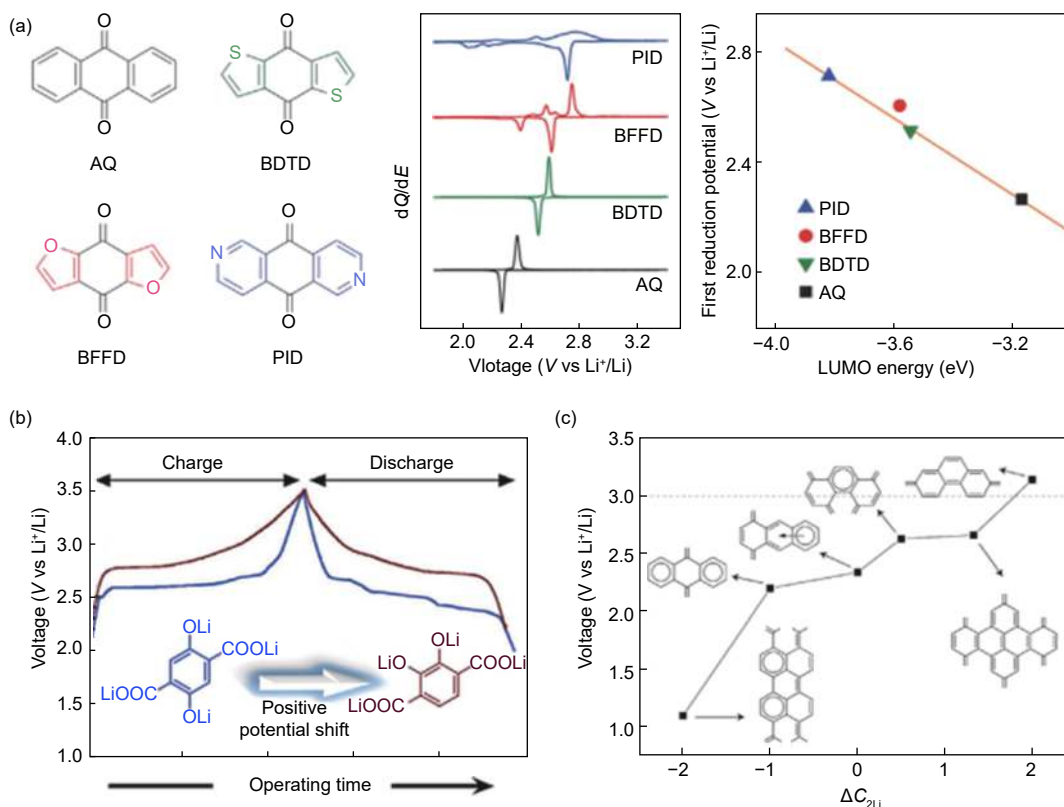


Fig. 5 The relationship between voltage and molecular structure: (a) small molecules as the cathode in a LIB: molecular structures, differential capacity curves and correlation between the first reduction potentials and the calculated LUMO energies<sup>[94]</sup>, (b) the effect of active sites position<sup>[95]</sup> and (c) conjugated structure<sup>[96]</sup> on voltage (a) Reproduced by permission of Wiley-VCH, (b) Reproduced by permission of American Chemical Society and (c) Reproduced by permission of the Royal Society of Chemistry.



(LUMO)<sup>[94, 97]</sup>, the amount<sup>[98]</sup> and relative position of active sites in the molecular<sup>[95, 99]</sup>. As shown in Fig. 5a, carbonyl-based electrode compounds were used as a cathode and coupled with a Li metal anode to fabricate a LIB<sup>[94]</sup>. It is found that redox potential (versus  $\text{Li}^{+/0}$ ) of small molecules in the LIB follows their trend of electron affinity that is reflected by their energy levels of LUMO. The lower LUMO of a small molecule gives rise to higher electron affinity, leading to a higher redox potential (first reduction potential in Fig. 5a). Besides, the molecular structure of redox organic cathode affects their voltage (versus  $\text{Li}^{+/0}$ ). For instance, switching from para to ortho-position in the quinone/hydroquinone moiety leads to the positive potential shift (Fig. 5b)<sup>[95]</sup>. Moreover, different conjugated small molecules with two carbonyl active sites show different voltages (versus  $\text{Li}^{+/0}$ ) (Fig. 5c)<sup>[96]</sup>. These results show that some of the operational characteristics of molecular electrode materials could be predictably engineered through rationally designing their molecular structures.

Moreover, the so-called p-type active sites such

as conjugated N-heterocycles<sup>[100]</sup>, which possess a high redox potential, can be incorporated into COFs to achieve a high voltage. Thanks to tunable structures, active units with different redox groups can be chosen as building blocks, giving various COFs that can serve as cathodes or anodes to fabricate RMBs with high working voltage. Obviously, high working voltage will be obtained by using a COF cathode with a high redox potential or a COF anode with a low redox potential, both of which can be prepared by molecular engineering. Thus, COFs hold great potential in both anode and cathode materials for RMBs.

### 3.2 Rate performance

Rate performance is the charge-discharge ability of electrode materials at different rates, which is essential to electronic and electrical devices, such as electrical cars. High-rate performance makes fast-charging electrical cars competitive with gasoline cars that can be refueled within 5 min (equivalent to 12 C for charging the RMBs)<sup>[101]</sup>. High-rate performance needs fast electron and ion transfer during charging/discharging processes, both of which can be realized

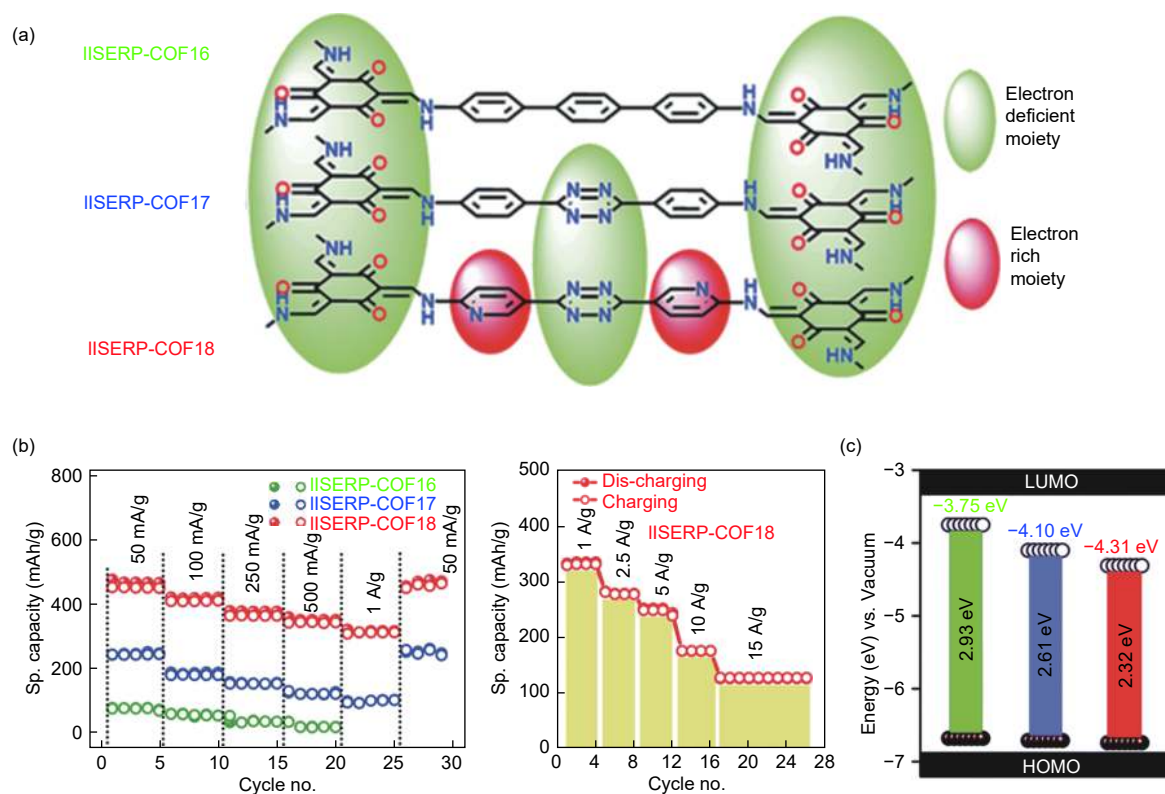


Fig. 6 (a) Different molecular configurations, (b) the electrochemical performance of three COFs, (c) the molecular orbital energy level of three different COFs<sup>[79]</sup> (Reproduced by permission of the Royal Society of Chemistry).

through tuning the structures of COF electrode materials. COFs usually suffer from poor electronic conductivity, however, which can be improved by adjusting intrinsic properties via optimizing their structures, such as optimizing their energy levels, extending conjugated structures, introducing active sites with fast redox kinetics, and hybridizing with conductive materials. Tunable porous structures endow COF electrode materials with plenty of channels, facilitating ion transportation—inefficient ion transfer often leads to low-rate performance and serious concentration overpotential in the high rate cycling process, decreasing RMBs' energy storage capacity<sup>[24, 102, 103]</sup>.

The electron transfer in COF electrode materials can be enhanced by tuning the molecular energy levels of COFs (Fig. 6)<sup>[79]</sup>. By controlling the number of nitrogen atoms at the linkers of a COF anode in sodium ion batteries, electron-rich moieties are created, which reduces the HOMO-LUMO gap of the molecular while keeps the HOMO constantly (Fig. 6c). According to the frontier molecular orbital theory, a narrower energy gap between HOMO-LUMO is beneficial to the activation of bonded electrons and benefits to the electronic conductivity<sup>[104–107]</sup>. In addition, it is proposed that electrons accumulate in the anti-bond-

ing LUMO when reducing the cell-potential, leading to electron-dosed LUMO levels that enable a COF anode to efficiently attract the sluggish sodium ions from the electrolyte. Consequently, as the ionic and electronic conductivity both increased, the COF anode in sodium ion batteries with the narrowest energy gap demonstrates the best rate performance, delivering a specific capacity of 128 mAh g<sup>-1</sup> at 15 A g<sup>-1</sup> (Fig. 6b).

Besides, the electronic conductivity can be also increased by extending the conjugated structure of COFs and delocalizing the  $\pi$  electrons in the whole crystalline 2D plane<sup>[64]</sup>. As shown in Fig. 7, via condensation of naphthylamide with different knots, Tp and Tb, two COF cathode materials for LIBs were fabricated. Compared to Tp-DANT-COF, Tb-DANT-COF shows faster kinetics and lower resistance of charge transfer and Warburg impedance because of its extended  $\pi$ -conjugated backbone. As a result, Tb-DANT-COF displays better electrochemical performance, especially rate performance (Fig. 7b). Meanwhile, the Tb-DANT-COF shows smaller redox potential difference in CV curves, meaning that the promotion of conjugation degree boosts the kinetic process (Fig. 7c and d).

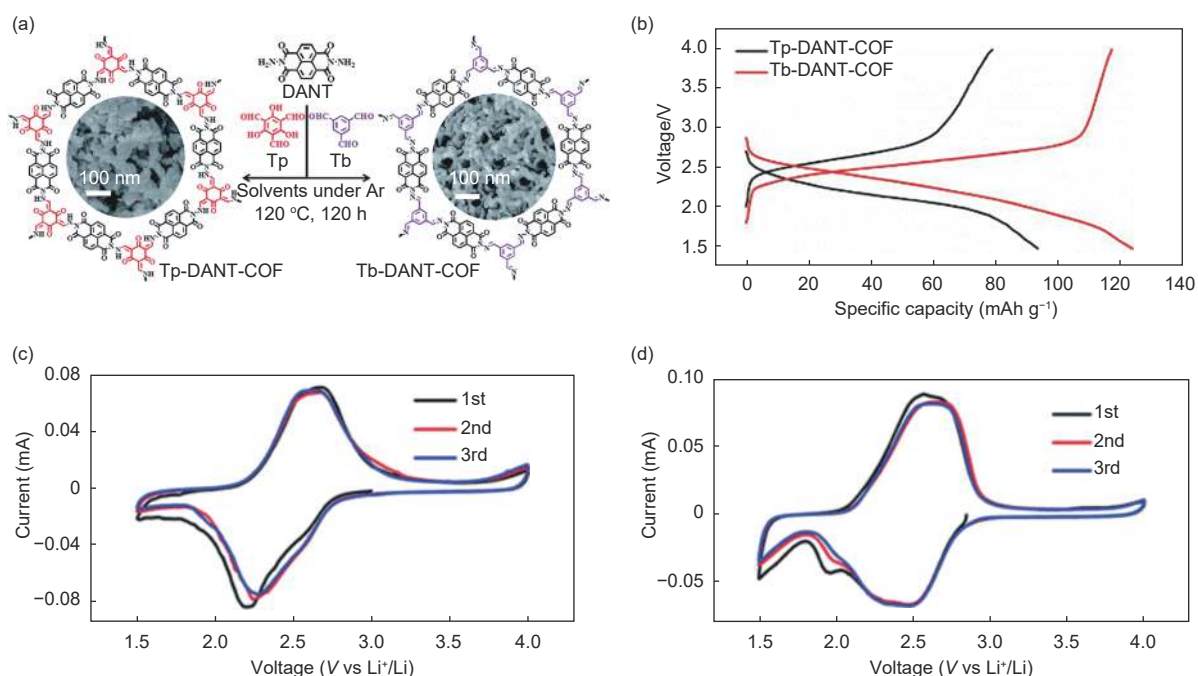


Fig. 7 (a) The microstructures of two COFs, (b) the specific capacity, the cyclic voltammetry curves for (c) Tp-DANT-COF and (d) Tb-DANT-COF<sup>[64]</sup> (Reproduced by permission of the Royal Society of Chemistry).

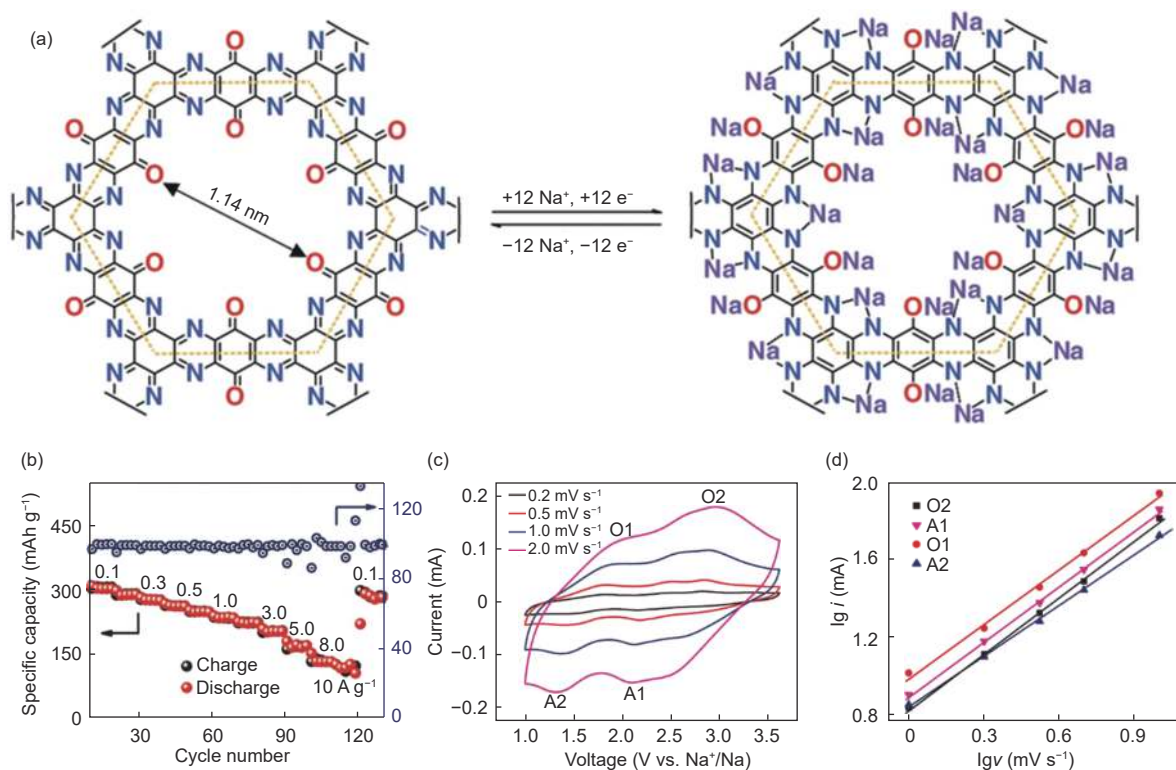


Fig. 8 (a) The structure of a nitrogen-rich COF, (b) the rate performance, (c) the cyclic voltammetry curves for the nitrogen-rich COF and (d)  $\lg i$ - $\lg v$  curves for the b evaluation<sup>[53]</sup> (Reproduced by permission of Nature Publishing Group).

Besides adjusting energy levels and conjugated structures of COF electrode materials, other methods such as hybridizing COFs with CNTs<sup>[59, 108]</sup> or graphene<sup>[54]</sup> are helpful to enhance electron conductivity as well, although it might decrease the gravimetric and volumetric capacity of electrodes.

The ion transfer of COF electrode materials can be enhanced by tuning their particle size and structures. As mentioned in Fig. 3<sup>[69]</sup>, the prepared rCTF are small size nanoparticles (50–100 nm) with progressively increased structural disorder, which increases the kinetics of infiltration and significantly shortens the activation period, yielding fast-charging Li-ion half and full cells even at a high-capacity loading. Additionally, adjusting the ion diffusion kinetics by rational synthesis of a COF is also an effective way to facilitate RMBs' power density. It is well known that when the  $b$  value in the equation  $i = av^b$  equals to 0.5, the kinetic process is under a diffusion-controlled mechanism while for  $b$  equals to 1, the mechanism is similar to supercapacitor behavior, in which surface control dominates<sup>[109]</sup>. As shown in Fig. 8, a nitrogen-

rich COF anode for sodium ion batteries possesses a  $b$  value close to 0.9 (evaluated from the CV curve and  $\lg i$ - $\lg v$  plot in Fig. 8c and d), indicating that it is governed by surface control and thus demonstrating a specific capacity of 134.3 mAh g<sup>-1</sup> (Fig. 8b) at a high current density of 10 A g<sup>-1</sup><sup>[53]</sup>. Moreover, other strategies such as exfoliating COFs into single or few-layer structure<sup>[58, 65, 66]</sup> have been also applied to increase the rate performance of COF electrode materials.

### 3.3 Cyclic lifespan

Cycling stability is also critical to organic electrode materials in RMBs, which are affected by volume change<sup>[110–112]</sup>, side reactions<sup>[113, 114]</sup>, phase transformation<sup>[115]</sup> and stability of intermediates<sup>[67]</sup>. In contrast, most COF electrode materials do not suffer for these issues on account of their robust covalent bonds, superior thermal<sup>[71]</sup> and chemical stability (Table 1)<sup>[78]</sup>. What's more, compared with conventional organic small molecules for RMBs, COF electrode materials exhibit better cycling stability because they have poor solubility in organic solvents<sup>[116, 117]</sup> and there are almost no structural instability problems in

COF electrodes caused by the serious volume change because of their intrinsic features as 2D materials<sup>[118]</sup>.

Above all, COF electrode materials that exhibit remarkable long-term stability need to possess robust

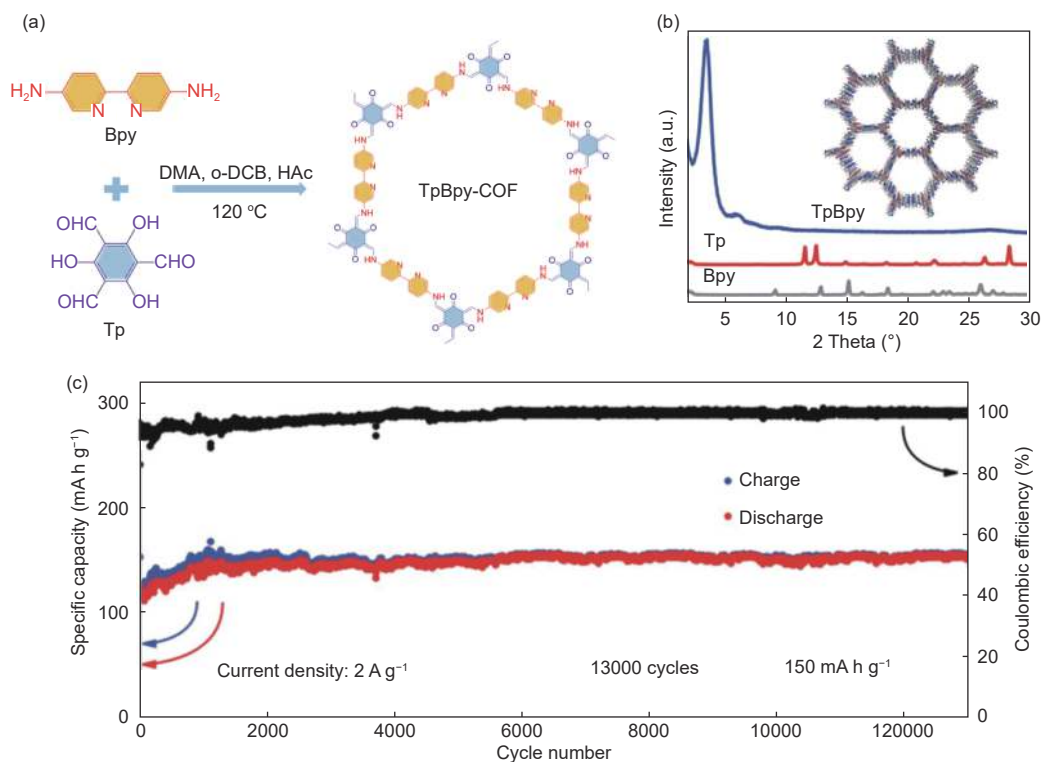


Fig. 9 (a) The synthetic route of TpBpy-COF, (b) the XRD pattern of TpBpy-COF and (c) cyclic performance of TpBpy-COF<sup>[84]</sup> (Reproduced by permission of Wiley-VCH).

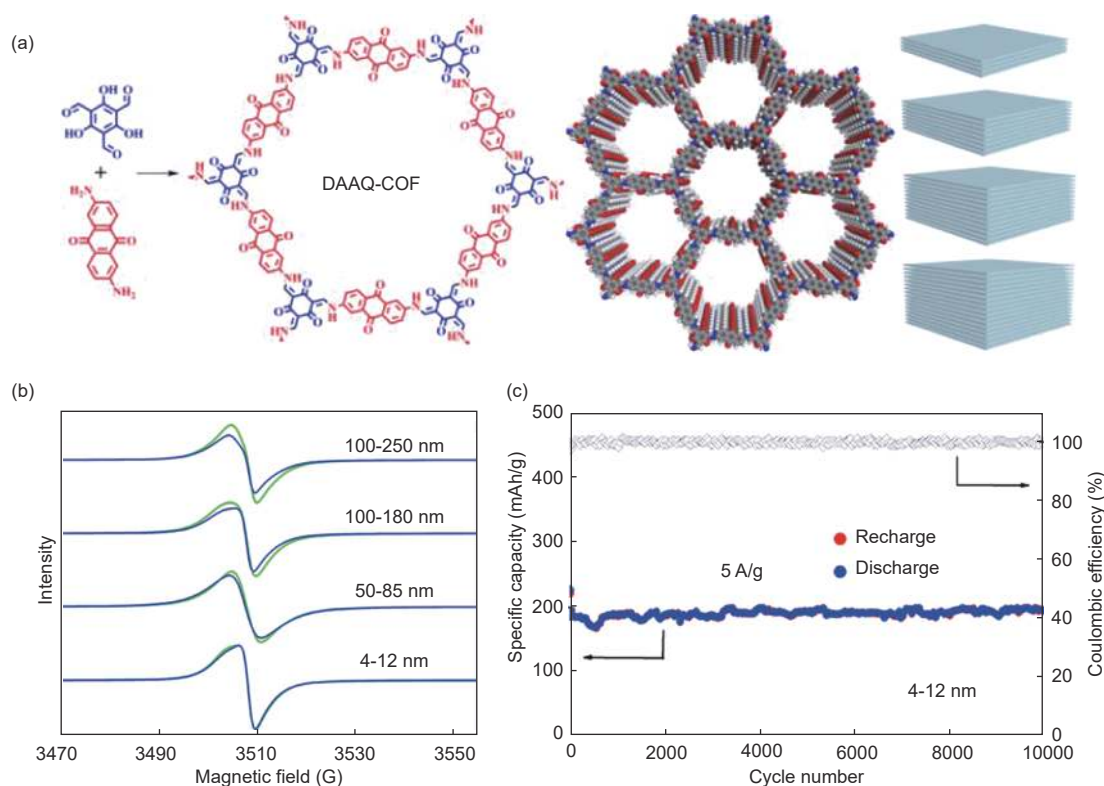


Fig. 10 (a) Structures of DAAQ-COF with different thicknesses, (b) change of EPR signal for COFs with different thicknesses and (c) the cyclic performance for DAAQ-COF with a thickness of 4-12 nm<sup>[67]</sup> (Reproduced by permission of American Chemical Society).



structures. As shown in Fig. 9, a COF containing 2,2'-bi-pyridine moieties (TpBpy-COF) for aluminum-ion batteries (AIBs) have highly crystalline and robust frameworks, which could maintain the structural integrity during the repeated intercalation/de-intercalation of anions, thus, delivering a 100% capacity retention

after 13 000 cycles between 0.01–2.3 V at  $2 \text{ A g}^{-1}$  [84]. Powder X-ray diffraction (PXRD) analysis shows that the COF electrodes before and after 13 000 cycles show comparable peaks at  $3.68^\circ$  with no extra peaks, confirming the retention of the robust COF framework structure after 13 000 cycles.

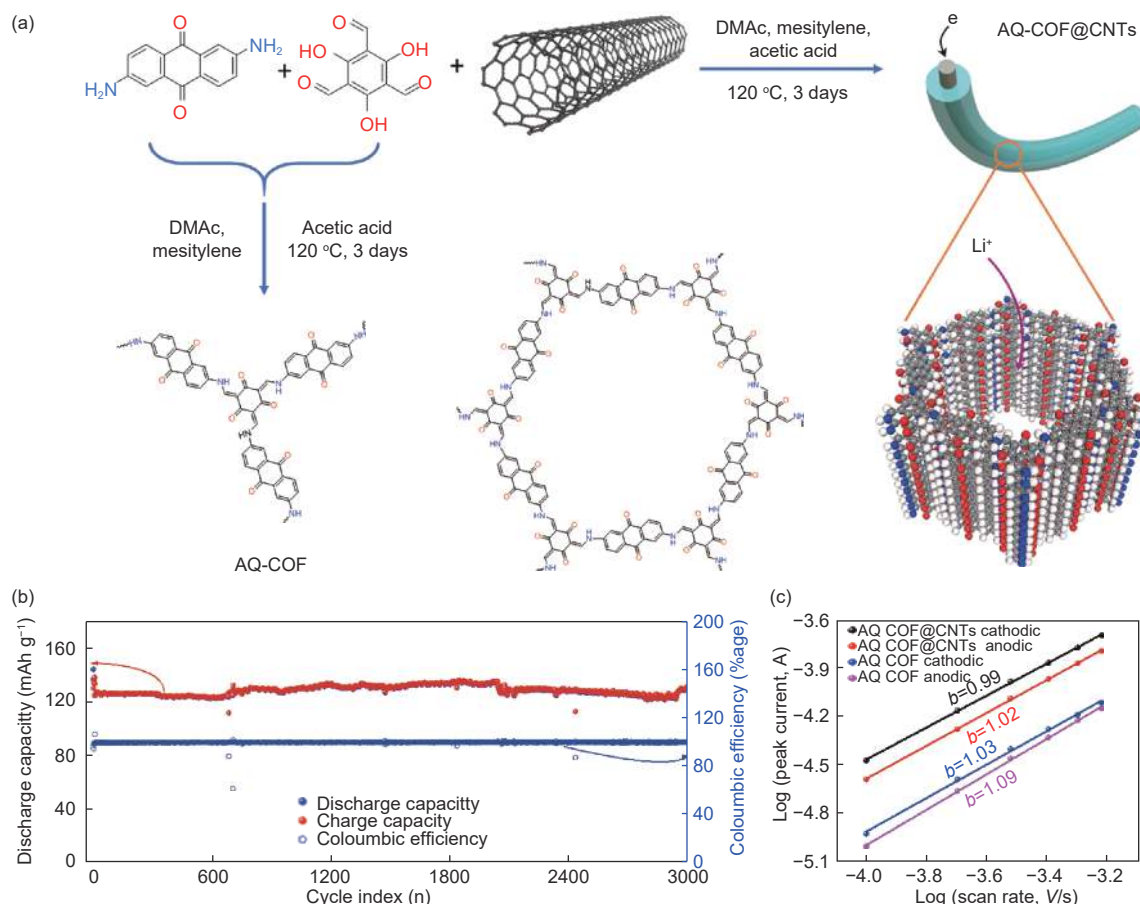


Fig. 11 (a) Synthesis of AQ-COF@CNTs, (b) the cyclic performance of AQ-COF@CNTs and (c)  $\lg i$ - $\lg v$  curves<sup>[75]</sup>  
(Reproduced by permission of the Royal Society of Chemistry).

Additionally, exfoliation is likewise a conducive approach to prolong the COF electrode cyclic lifespan<sup>[67]</sup>. As shown in Fig. 10, as the thickness of 2D COF nanosheets decreases, the stability of intermediates will be enhanced as detected by the means of electron paramagnetic resonance (Fig. 10b), promoting the electrochemical performance. Consequently, the electrodes with the thinnest COF (around 4–12 nm) exhibit the best cycling performance of a 99% capacity retention after 10 000 cycles (Fig. 10c). Moreover, it has been proved that the ion diffusion will also be improved after exfoliation treatment<sup>[66]</sup>, which

benefits the electrochemical reactivity and thus contributes to cycling stability.

Moreover, the surface-controlled pseudo-capacitive reactions in COF electrode can be advantageous to boost RBMs' cycling life as well<sup>[5]</sup>. For instance, after the COF is hybridized with CNTs, the cycling stability of AQ-COF electrode in LIBs are significantly improved—the AQ-COF@CNT electrode demonstrates nearly no capacity drop after 3 000 cycles (Fig. 11b). It is found that CNTs do not bring about additional specific capacity obviously to the AQ-COF, but they induce high specific surface area with high porosity

and good electrical conductivity, and thus induce a surface-controlled pseudocapacitive energy storage mechanism (characteristic of supercapacitors), leading to good rate performance and outstanding long cyclic life.

In addition, it is also necessary to pay special attention to redox groups in COF electrode materials. Evidently, redox groups with highly reversible redox behaviors benefit cycle life of COFs because they will enable COFs to maintain high Coulombic efficiency in each cycle. Besides, the redox groups need to remain stable during charging/discharging processes.

## 4 Summaries and perspectives

Apparently, COFs are highly promising electrode materials for RMBs because of their unique features, including the plentiful and diversiform active sites, the light-weight element composition, the tunable channels for ion transfer and adjustable molecular structure to achieve a high voltage. All these features endow COFs with huge potential in providing high energy densities as electrode materials. Furthermore, their ionic and electronic conductivity can be improved by tuning their pore size, enhancing the rate performance and cyclic lifespan. In addition, the robust 2D frameworks constituted of covalent bonds, and the insolubility in the organic electrolyte guarantee the stability of COF electrodes, which ensure their long cyclic lifespan in RMBs as well.

Although significant progress has been achieved, there are still some problems in COF electrode materials that should be addressed, including poor electronic conductivity, low volumetric energy density, complex synthesis, and obscure mechanism. Thus, to overcome these problems hindering the development of COFs in RMBs, several strategies are proposed. 1) Heteroatoms, such as B, S, and P, should be tried to be incorporated into COFs to tune their electronic structures, consequently, improving their electronic conductivity or achieving higher voltages. Besides, the electronic conductivity of COF electrode materials would be also improved by extending the conjugation of their framework. Fully  $\pi$ -conjugated frame-

works should endow COFs with higher conductivity. Therefore, aromatic rings, such as benzene, naphthalene, anthracene, and pyrene, are highly promising building blocks for construction of COFs; 2) Other efficient redox groups besides amides, quinones and imine should be considered to achieve high volumetric energy density when fabricating COF electrode materials. Additionally, the number of active sites in COFs should be increased to enhance their specific capacity and thus improve their volumetric energy density; 3) The synthesis of COFs should be simplified by rational design of their structures and building blocks; 4) The mechanism of charge storage in aromatic rings needs to be further explored, which is still under intensive debate; 5) COFs have been hybridized with CNT, graphene,  $\text{MnO}_2$  and silicon (Table 1). Thus, conventional active materials, such as  $\text{LiFePO}_4$ ,  $\text{LiCoO}_2$ ,  $\text{LiMn}_2\text{O}_4$ , and  $\text{V}_2\text{O}_5$ , should be also considered to be hybridized with COFs to obtain high performance COF-based composites because both of COFs and active materials would contribute to the electrochemical performance of composites.

## Acknowledgements

The Authors would like to offer special thanks to National Natural Science Foundation of China (51425302, 51302045) and the Beijing Natural Science Foundation (2182086).

## References

- [1] Dunn B, Kamath H, Tarascon J. Electrical energy storage for the grid: A battery of choices[J]. *Science*, 2011, 334(6058): 928.
- [2] Lukatskaya M, Dunn B, Gogotsi Y. Multidimensional materials and device architectures for future hybrid energy storage[J]. *Nature Communications*, 2016, 7(1): 12647.
- [3] Wang L, Chen B, Ma J, et al. Reviving lithium cobalt oxide-based lithium secondary batteries-toward a higher energy density[J]. *Chemical Society Reviews*, 2018, 47(17): 6505-6602.
- [4] Wang Z, Jin W, Huang X, et al. Covalent organic frameworks as electrode materials for metal ion batteries: A current review[J]. *The Chemical Record*, 2020, 20(10): 1198-1219.
- [5] Wen Y, Wang X, Yang Y, et al. Covalent organic framework-regulated ionic transportation for high-performance lithium-ion batteries[J]. *Journal of Materials Chemistry A*, 2019, 7(46): 26540-26548.
- [6] Hwang J, Myung S, Sun Y. Sodium-ion batteries: Present and future[J]. *Chemical Society Reviews*, 2017, 46: 3529-3614.

- [ 7 ] Song M, Tan H, Chao D, et al. Recent advances in Zn-ion batteries[J]. *Advanced Functional Materials*, 2018, 28(41): 1802564.
- [ 8 ] Muldoon J, Bucur C, Oliver A, et al. Electrolyte roadblocks to a magnesium rechargeable battery[J]. *Energy & Environmental Science*, 2012, 5: 5941.
- [ 9 ] Wu X, Leonard D, Ji X. Emerging non-aqueous potassium-ion batteries: Challenges and opportunities[J]. *Chemistry of Materials*, 2017, 29: 5031-5042.
- [ 10 ] Wang M, Jiang C, Zhang S, et al. Reversible calcium alloying enables a practical room-temperature rechargeable calcium-ion battery with a high discharge voltage[J]. *Nature Chemistry*, 2018, 10(6): 667-672.
- [ 11 ] Zhang Y, Liu S, Ji Y, et al. Emerging nonaqueous aluminum-ion on batteries: Challenges, status, and perspectives[J]. *Advanced Materials*, 2018, 30: 1706310.
- [ 12 ] Nishi Y. Lithium ion secondary batteries; past 10 years and the future[J]. *Journal of Power Sources*, 2001, 100: 101-106.
- [ 13 ] Li M, Lu J, Chen Z, et al. 30 Years of lithium-ion batteries[J]. *Advanced Materials*, 2018, 30: 1800561.
- [ 14 ] Ozawa K. Lithium-ion rechargeable batteries with LiCoO<sub>2</sub> and carbon electrodes: The LiCoO<sub>2</sub>/C system[J]. *Solid State Ionics Diffusion & Reactions*, 1994, 69: 212-221.
- [ 15 ] Jiang Q, Han Z, Wang S. Plasma-enhanced low-temperature solid-state synthesis of spinel LiMn<sub>2</sub>O<sub>4</sub> with superior performance for lithium-ion batteries[J]. *Green Chemistry*, 2016, 18: 662-666.
- [ 16 ] Prosini P. Iron Phosphate Materials as Cathodes for Lithium Batteries [M]. Italy: Springer, 2011, 73-82.
- [ 17 ] Yoshio M, Wang H, Fukuda K, et al. Effect of carbon coating on electrochemical performance of treated natural graphite as lithium-ion battery anode material[J]. *Journal of the Electrochemical Society*, 2000, 147(4): 1245-1250.
- [ 18 ] Lee H, Baek J, Lee S, et al. Effect of carbon coating on elevated temperature performance of graphite as lithium-ion battery anode material[J]. *Journal of Power Sources*, 2004, 128(1): 61-66.
- [ 19 ] Son I, Hwan Park J, Kwon S, et al. Silicon carbide-free graphene growth on silicon for lithium-ion battery with high volumetric energy density[J]. *Nature Communications*, 2015, 6: 7393.
- [ 20 ] Zuo X, Zhu J, Müller-Buschbaum P, et al. Silicon based lithium-ion battery anodes: A chronicle perspective review[J]. *Nano Energy*, 2017, 31: 113-143.
- [ 21 ] Zhang X, Wang D, Qiu X, et al. Stable high-capacity and high-rate silicon-based lithium battery anodes upon two-dimensional covalent encapsulation[J]. *Nature Communications*, 2020, 11(1): 3826.
- [ 22 ] Zeng X, Zhan C, Lu J, et al. Stabilization of a high-capacity and high-power nickel-based cathode for Li-ion batteries[J]. *Chem*, 2018, 4(4): 690-704.
- [ 23 ] Xing Z, Wang S, Yu A, et al. Aqueous intercalation-type electrode materials for grid-level energy storage: Beyond the limits of lithium and sodium[J]. *Nano Energy*, 2018, 50: 229-244.
- [ 24 ] Goodenough J, Park K. The Li-ion rechargeable battery: A perspective[J]. *Journal of the American Chemical Society*, 2013, 135(4): 1167-1176.
- [ 25 ] Wang Y, He P, Zhou H. A lithium-air capacitor-battery based on a hybrid electrolyte[J]. *Energy & Environmental Science*, 2011, 4(12): 4994-4999.
- [ 26 ] Braun P, Cho J, Pikul J, et al. High power rechargeable batteries[J]. *Current Opinion in Solid State and Materials Science*, 2012, 16(4): 186-198.
- [ 27 ] Guerfi A, Trottier J, Boyano I, et al. High cycling stability of zinc-anode/conducting polymer rechargeable battery with non-aqueous electrolyte[J]. *Journal of Power Sources*, 2014, 248(15): 1099-1104.
- [ 28 ] Zhibin L, Chong Q, Wenhan G, et al. Metal-organic frameworks: pristine metal-organic frameworks and their composites for energy storage and conversion[J]. *Advanced Materials*, 2018, 30(37): 1870276.
- [ 29 ] Chen N, Zhang H, Li L, et al. Ionogel electrolytes for high - performance lithium batteries: A review[J]. *Advanced Energy Materials*, 2018, 8(12): 1702675.
- [ 30 ] Wang F, Wu X, Yuan X, et al. Latest advances in supercapacitors: From new electrode materials to novel device designs[J]. *Chemical Society Reviews*, 2017, 46(22): 6816-6854.
- [ 31 ] Medina D, Sick T, Bein T. Photoactive and conducting covalent organic frameworks[J]. *Advanced Energy Materials*, 2017, 7(16): 1700387.
- [ 32 ] Pachfule P, Acharjya A, Roeser J, et al. Diacetylene functionalized covalent organic framework (COF) for photocatalytic hydrogen generation[J]. *Journal of the American Chemical Society*, 2017, 140(4): 1423-1427.
- [ 33 ] Lin C, Zhang L, Zhao Z, et al. Design principles for covalent organic frameworks as efficient electrocatalysts in clean energy conversion and green oxidizer production[J]. *Advanced Materials*, 2017, 29(17): 1606635.
- [ 34 ] Wu D, Xu Q, Jing Q, et al. Bimetallic covalent organic frameworks for constructing multifunctional electrocatalyst[J]. *Chemistry*, 2019, 26: 3105-3111.
- [ 35 ] Yang S, Hu W, Zhang X, et al. 2D covalent organic frameworks as intrinsic photocatalysts for visible light-driven CO<sub>2</sub> reduction[J]. *Journal of the American Chemical Society*, 2018, 140(44): 14614-14618.
- [ 36 ] Fan H, Mundstock A, Feldhoff A, et al. Covalent organic framework-covalent organic framework bilayer membranes for highly selective gas separation[J]. *Journal of the American Chemical Society*, 2018, 140: 10094-10098.
- [ 37 ] Fu J, Das S, Xing G, et al. Fabrication of COF-MOF composite membranes and their highly selective separation of H<sub>2</sub>/CO<sub>2</sub>[J]. *Journal of the American Chemical Society*, 2016, 138(24): 7673-7680.
- [ 38 ] Kang Z, Peng Y, Qian Y, et al. Mixed matrix membranes (MMMs) comprising exfoliated 2D covalent organic frameworks (COFs) for efficient CO<sub>2</sub> separation[J]. *Chemistry of Materials*, 2016, 28(5): 1277-1285.
- [ 39 ] Alhmod H, Delalat B, Elnathan R, et al. Porous silicon nanodiscs for targeted drug delivery[J]. *Advanced Functional Materials*, 2015, 25(7): 1137-1145.
- [ 40 ] Zhang G, Li X, Liao Q, et al. Water-dispersible PEG-curcumin/amine-functionalized covalent organic framework nanocomposites as smart carriers for in vivo drug delivery[J].

- Nature Communications*, 2018, 9: 2785.
- [41] Rosi N. Hydrogen storage in microporous metal-organic frameworks[J]. *Science*, 2003, 300(5622): 1127-1129.
- [42] Furukawa H, Yaghi O. Storage of hydrogen, methane, and carbon dioxide in highly porous covalent organic frameworks for clean energy applications[J]. *Journal of the American Chemical Society*, 2009, 131(25): 8875-8883.
- [43] Geng K, He T, Liu R, et al. Covalent organic frameworks: Design, synthesis, and functions[J]. *Chemical Reviews*, 2020, 120: 8814-8933.
- [44] Côté Adrien P, Benin Annabelle I, Ockwig Nathan W, et al. Porous, crystalline, covalent organic frameworks[J]. *Science*, 2005, 310(5751): 1166-1170.
- [45] Feng X, Ding X, Jiang D. Covalent organic frameworks[J]. *Chemical Society Reviews*, 2012, 41(18): 6010-6022.
- [46] Sun T, Xie J, Guo W, et al. Covalent-organic frameworks: Advanced organic electrode materials for rechargeable batteries[J]. *Advanced Energy Materials*, 2020, 10: 1904199.
- [47] Huang N, Wang P, Jiang D. Covalent organic frameworks: A materials platform for structural and functional designs[J]. *Nature Reviews Materials*, 2016, 1: 16068.
- [48] Geng K, Arumugam V, Xu H, et al. Covalent organic frameworks: Polymer chemistry and functional design[J]. *Progress in Polymer Science*, 2020, 108: 101288.
- [49] Yusran Y, Fang Q, Valtchev V. Electroactive covalent organic frameworks: Design, synthesis, and applications[J]. *Advanced Materials*, 2020, 32: 2002038.
- [50] Hu Y, Wayment L, Haslam C, et al. Covalent organic framework based lithium-ion battery: Fundamental, design and characterization[J]. *EnergyChem*, 2020, 3(1): 100048.
- [51] Xiao Z, Li L, Tang Y, et al. Covalent organic frameworks with lithiophilic and sulfiphilic dual linkages for cooperative affinity to polysulfides in lithium-sulfur batteries[J]. *Energy Storage Materials*, 2018, 12: 252-259.
- [52] Xu F, Jin S, Zhong H, et al. Electrochemically active, crystalline, mesoporous covalent organic frameworks on carbon nanotubes for synergistic lithium-ion battery energy storage[J]. *Scientific Reports*, 2015, 5(1): 8225.
- [53] Shi R, Liu L, Lu Y, et al. Nitrogen-rich covalent organic frameworks with multiple carbonyls for high-performance sodium batteries[J]. *Nature Communications*, 2020, 11(1): 178.
- [54] Luo Z, Liu L, Ning J, et al. A microporous covalent organic framework with abundant accessible carbonyl groups for lithium-ion batteries[J]. *Angewandte Chemie International Edition*, 2018, 57(30): 9443-9446.
- [55] Xu S, Wang G, Biswal B, et al. A nitrogen-rich 2D sp<sup>2</sup>-carbon-linked conjugated polymer framework as a high-performance cathode for lithium-ion batteries[J]. *Angewandte Chemie International Edition*, 2018, 131(1): 859-863.
- [56] Khayum M, Ghosh M, Vijayakumar V, et al. Zinc ion interactions in a two-dimensional covalent organic framework based aqueous zinc ion battery[J]. *Chemical Science*, 2019, 10(38): 8889-8894.
- [57] Lei Z, Yang Q, Xu Y, et al. Boosting lithium storage in covalent organic framework via activation of 14-electron redox chemistry[J]. *Nature Communications*, 2018, 9(1): 576.
- [58] Lei Z, Chen X, Sun W, et al. Exfoliated triazine-based covalent organic nanosheets with multielectron redox for high-performance lithium organic batteries[J]. *Advanced Energy Materials*, 2018, 9(3): 1801010.
- [59] Chen X, Zhang H, Ci C, et al. Few-layered boronic ester based covalent organic frameworks/carbon nanotube composites for high-performance K-organic batteries[J]. *ACS Nano*, 2019, 13(3): 3600-3607.
- [60] Yang H, Zhang S, Han L, et al. High conductive two-dimensional covalent organic framework for lithium storage with large capacity[J]. *ACS Applied Materials & Interfaces*, 2016, 8(8): 5366-5375.
- [61] Zhang H, Sun W, Chen X, et al. Few-layered fluorinated triazine-based covalent organic nanosheets for high-performance alkali organic batteries[J]. *ACS Nano*, 2019, 13(12): 14252-14261.
- [62] Yang X, Hu Y, Dunlap N, et al. A truxenone-based covalent organic framework as all-solid-state Li-ion battery cathode with high capacity[J]. *Angewandte Chemie International Edition*, 2020, 59(46): 20385-20389.
- [63] Sakaushi K, Hosono E, Nickerl G, et al. Aromatic porous-honeycomb electrodes for a sodium-organic energy storage device[J]. *Nature Communications*, 2013, 4(1): 1485.
- [64] Yang D, Yao Z, Wu D, et al. Structure-modulated crystalline covalent organic frameworks as high-rate cathodes for Li-ion batteries[J]. *Journal of Materials Chemistry A*, 2016, 4(47): 18621-18627.
- [65] Wang Z, Li Y, Liu P, et al. Few layer covalent organic frameworks with graphene sheets as cathode materials for lithium-ion batteries[J]. *Nanoscale*, 2019, 11(12): 5330-5335.
- [66] Wang S, Wang Q, Shao P, et al. Exfoliation of covalent organic frameworks into few-layer redox-active nanosheets as cathode materials for lithium-ion batteries[J]. *Journal of the American Chemical Society*, 2017, 139(12): 4258-4261.
- [67] Gu S, Wu S, Cao L, et al. Tunable redox chemistry and stability of radical intermediates in 2D covalent organic frameworks for high performance sodium ion batteries[J]. *Journal of the American Chemical Society*, 2019, 141(24): 9623-9628.
- [68] Bai L, Gao Q, Zhao Y. Two fully conjugated covalent organic frameworks as anode materials for lithium ion batteries[J]. *Journal of Materials Chemistry A*, 2016, 4(37): 14106-14110.
- [69] Buyukcakir O, Ryu J, Joo S, et al. Lithium accommodation in a redox-active covalent triazine framework for high areal capacity and fast-charging lithium-ion batteries[J]. *Advanced Functional Materials*, 2020, 30(36): 2003761.
- [70] Patra B, Das S, Ghosh A, et al. Covalent organic framework based microspheres as an anode material for rechargeable sodium batteries[J]. *Journal of Materials Chemistry A*, 2018, 6(34): 16655-16663.
- [71] Wu M, Zhao Y, Sun B, et al. A 2D covalent organic framework as a high-performance cathode material for lithium-ion batteries[J]. *Nano Energy*, 2020, 70: 104498.
- [72] Xu J, Mahmood J, Dou Y, et al. 2D frameworks of C<sub>2</sub>N and C<sub>3</sub>N as new anode materials for lithium-ion batteries[J]. *Advanced Materials*, 2017, 29(34): 1702007.
- [73] Li X, Wang H, Chen H, et al. Dynamic covalent synthesis of



- crystalline porous graphitic frameworks[J]. *Chem*, 2020, 6(4): 933-944.
- [ 74 ] Wolfson E, Xiao N, Schkeryantz L, et al. A dehydrobenzoannulene-based two-dimensional covalent organic framework as an anode material for lithium-ion batteries[J]. *Molecular Systems Design & Engineering*, 2020, 5(1): 97-101.
- [ 75 ] Amin K, Zhang J, Zhou H, et al. Surface controlled pseudo-capacitive reactions enabling ultra-fast charging and long-life organic lithium ion batteries[J]. *Sustainable Energy & Fuels*, 2020, 4(8): 4179-4185.
- [ 76 ] Yu X, Li C, Ma Y, et al. Crystalline, porous, covalent polyoxometalate-organic frameworks for lithium-ion batteries[J]. *Microporous and Mesoporous Materials*, 2020, 299: 110105.
- [ 77 ] Xu F, Chen X, Tang Z, et al. Redox-active conjugated microporous polymers: A new organic platform for highly efficient energy storage[J]. *Chemical Communications*, 2014, 50(37): 4788-4790.
- [ 78 ] Halder S, Roy K, Nandi S, et al. High and reversible lithium ion storage in self-exfoliated triazole-triformyl phloroglucinol-based covalent organic nanosheets[J]. *Advanced Energy Materials*, 2018, 8(8): 1702170.
- [ 79 ] Halder S, Kaleeswaran D, Rase D, et al. Tuning the electronic energy level of covalent organic frameworks for crafting high-rate Na-ion battery anode[J]. *Nanoscale Horizons*, 2020, 5(8): 1264-1273.
- [ 80 ] Chen H, Zhang Y, Xu C, et al. Two  $\pi$ -conjugated covalent organic frameworks with long-term cyclability at high current density for lithium ion battery[J]. *Chemistry A European Journal*, 2019, 25(68): 15472-15476.
- [ 81 ] Zhang Y, Gao Z. High performance anode material for sodium-ion batteries derived from covalent-organic frameworks[J]. *Electrochimica Acta*, 2019, 301: 23-28.
- [ 82 ] Feng S, Xu H, Zhang C, et al. Bicarbazole-based redox-active covalent organic frameworks for ultrahigh-performance energy storage[J]. *Chemical Communications*, 2017, 53(82): 11334-11337.
- [ 83 ] Zhao G, Zhang Y, Gao Z, et al. Dual active site of the Azo and Carbonyl-modified covalent organic framework for high-performance Li storage[J]. *ACS Energy Letters*, 2020, 5(4): 1022-1031.
- [ 84 ] Lu H, Ning F, Jin R, et al. Two-dimensional covalent organic frameworks with enhanced aluminum storage properties[J]. *ChemSusChem*, 2020, 13(13): 3447-3454.
- [ 85 ] Li S, Li W, Wu X, et al. Pore-size dominated electrochemical properties of covalent triazine frameworks as anode materials for K-ion batteries[J]. *Chemical Science*, 2019, 10(33): 7695-7701.
- [ 86 ] Li H, Tang M, Wu Y, et al. Large  $\pi$ -conjugated porous frameworks as cathodes for sodium-ion batteries[J]. *The Journal of Physical Chemistry Letters*, 2018, 9(12): 3205.
- [ 87 ] Schon T, Tilley A, Kynaston E, et al. Three-dimensional arylene diimide frameworks for highly stable lithium ion batteries[J]. *ACS Applied Materials & Interfaces*, 2017, 9(18): 15631.
- [ 88 ] Chen X, Li Y, Wang L, et al. High-lithium-affinity chemically exfoliated 2D covalent organic frameworks[J]. *Advanced Materials*, 2019, 31(29): 1901640.
- [ 89 ] Ai Q, Fang Q, Liang J, et al. Lithium-conducting covalent-organic-frameworks as artificial solid-electrolyte-interphase on silicon anode for high performance lithium ion batteries[J]. *Nano Energy*, 2020, 72: 104657.
- [ 90 ] Wu F, Tan G, Chen R, et al. Novel solid-state Li/LiFePO<sub>4</sub> battery configuration with a ternary nanocomposite electrolyte for practical applications[J]. *Advanced Materials*, 2011, 23(43): 5081-5085.
- [ 91 ] Luo S, Wang K, Wang J, et al. Binder-free LiCoO<sub>2</sub>/carbon nanotube cathodes for high-performance lithium ion batteries[J]. *Advanced Materials*, 2012, 24(17): 2294-2298.
- [ 92 ] Jung Y, Lu P, Cavanagh A, et al. Unexpected improved performance of ALD coated LiCoO<sub>2</sub>/graphite Li-ion batteries[J]. *Advanced Energy Materials*, 2013, 3(2): 213-219.
- [ 93 ] Shim J, Lee S, Park S. Effects of MgO coating on the structural and electrochemical characteristics of LiCoO<sub>2</sub> as cathode materials for lithium ion battery[J]. *Chemistry of Materials*, 2014, 26(8): 2537-2543.
- [ 94 ] Liang Y, Zhang P, Yang S, et al. Fused heteroaromatic organic compounds for high-power electrodes of rechargeable lithium batteries[J]. *Advanced Energy Materials*, 2013, 3(5): 600-605.
- [ 95 ] Gottis S, Barrès A, Dolhem F, et al. Voltage gain in lithiated enolate-based organic cathode materials by isomeric effect[J]. *ACS Applied Materials & Interfaces*, 2014, 6(14): 10870-10876.
- [ 96 ] Wu D, Xie Z, Zhou Z, et al. Designing high-voltage carbonyl-containing polycyclic aromatic hydrocarbon cathode materials for Li-ion batteries guided by Clar's theory[J]. *Journal of Materials Chemistry A*, 2015, 3(37): 19137-19143.
- [ 97 ] Lu Y, Zhang Q, Li L, et al. Design strategies toward enhancing the performance of organic electrode materials in metal-ion batteries[J]. *Chem*, 2018, 4(12): 2786-2813.
- [ 98 ] Kim H, Kwon J, Lee B, et al. High energy organic cathode for sodium rechargeable batteries[J]. *Chemistry of Materials*, 2015, 27(21): 7258-7264.
- [ 99 ] Patil N, Aqil A, Ouhib F, et al. Bioinspired redox-active catechol-bearing polymers as ultrarobust organic cathodes for lithium storage[J]. *Advanced Materials*, 2017, 29(40): 1703373.
- [ 100 ] Lu Y, Chen J. Prospects of organic electrode materials for practical lithium batteries[J]. *Nature Reviews Chemistry*, 2020, 4(3): 127-142.
- [ 101 ] Schmuch R, Wagner R, Hörpel G, et al. Performance and cost of materials for lithium-based rechargeable automotive batteries[J]. *Nature Energy*, 2018, 3(4): 267-278.
- [ 102 ] Pramudita J, Sehwat D, Goonetilleke D, et al. An initial review of the status of electrode materials for potassium-ion batteries[J]. *Advanced Energy Materials*, 2017, 7(24): 1602911.
- [ 103 ] Kim S, Seo D, Ma X, et al. Electrode materials for rechargeable sodium-ion batteries: Potential alternatives to current lithium-ion batteries[J]. *Advanced Energy Materials*, 2012, 2(7): 710-721.
- [ 104 ] Zhang C, Qiao Y, Xiong P, et al. Conjugated microporous polymers with tunable electronic structure for high-performance potassium-ion batteries[J]. *ACS Nano*, 2019, 13(1): 745-754.
- [ 105 ] Song Z, Zhan H, Zhou Y. Polyimides: Promising energy-storage materials[J]. *Angewandte Chemie International Edition*, 2010, 49(45): 8444-8448.

- [106] Wang Orcid J, Chen C, Zhang Y. Hexaazatrinaphthylene-based porous organic polymers as organic cathode materials for lithium-ion batteries[J]. *ACS Sustainable Chemistry & Engineering*, 2018, 6(2): 1772-1779.
- [107] Wang J, Lee Y, Tee K, et al. A nanoporous sulfur-bridged hexaazatrinaphthylene framework as an organic cathode for lithium ion batteries with well-balanced electrochemical performance[J]. *Chemical Communications*, 2018, 54(55): 7681-7684.
- [108] Ye X, Huang Y, Tang X, et al. Two-dimensional extended  $\pi$ -conjugated triphenylene-core covalent organic polymer[J]. *Journal of Materials Chemistry A*, 2019, 7(7): 3066-3071.
- [109] Kou Y, Xu Y, Guo Z, et al. Supercapacitive energy storage and electric power supply using an Aza-fused  $\pi$ -conjugated microporous framework[J]. *Angewandte Chemie International Edition*, 2011, 123(37): 8912-8916.
- [110] Kim H, Seo D, Yoon G, et al. The reaction mechanism and capacity degradation model in lithium insertion organic cathodes,  $\text{Li}_2\text{C}_6\text{O}_6$ , using combined experimental and first principle studies[J]. *The Journal of Physical Chemistry Letters*, 2014, 5(17): 3086-3092.
- [111] Wang Y, Ding Y, Pan L, et al. Understanding the size-dependent sodium storage properties of  $\text{Na}_2\text{C}_6\text{O}_6$ -based organic electrodes for sodium-ion batteries[J]. *Nano Letters*, 2016, 16(5): 3329-3334.
- [112] Luo C, Fan X, Ma Z, et al. Self-healing chemistry between organic material and binder for stable sodium-ion batteries[J]. *Chem*, 2017, 3(6): 1050-1062.
- [113] Iordache A, Delhorbe V, Bardet M, et al. Perylene-based all-organic redox battery with excellent cycling stability[J]. *ACS Applied Materials & Interfaces*, 2016, 8(35): 22762-22767.
- [114] Shi Y, Tang H, Jiang S, et al. Understanding the electrochemical properties of naphthalene diimide: implication for stable and high-rate lithium-ion battery electrodes[J]. *Chemistry of Materials*, 2018, 30(10): 3508-3517.
- [115] Kundu D, Oberholzer P, Glaros C, et al. Organic cathode for aqueous Zn-ion batteries: Taming a unique phase evolution toward stable electrochemical cycling[J]. *Chemistry of Materials*, 2018, 30(11): 3874-3881.
- [116] Song Z, Qian Y, Gordin M, et al. Polyanthraquinone as a reliable organic electrode for stable and fast lithium storage[J]. *Angewandte Chemie International Edition*, 2015, 127(47): 14153-14157.
- [117] Muench S, Wild A, Friebe C, et al. Polymer-based organic batteries[J]. *Chemical Reviews*, 2016, 116(16): 9438-9484.
- [118] Fang L, Cao X, Cao Z. Covalent organic framework with high capacity for the lithium ion battery anode: Insight into intercalation of Li from first-principles calculations[J]. *Journal of Physics: Condensed Matter*, 2019, 31(20): 205502.

## 用于可充电金属离子电池的共价有机框架电极材料综述

曾术茂<sup>1,2,†</sup>, 黄小雄<sup>1,2,†</sup>, 马英杰<sup>1,\*</sup>, 智林杰<sup>1,2,\*</sup>

(1. 国家纳米科学中心, 纳米科学卓越创新中心, 纳米系统与多级次制造重点实验室, 北京 100190;

2. 中国科学院大学, 北京 100049)

**摘 要:** 共价有机框架具有强健的骨架、丰富的电化活性位点、便于金属离子传输的可控孔道以及利于优化电化性能的可调控的分子结构, 因此是理想的下一代可充电金属离子电池电极材料。此外, 共价有机框架电极材料没有传统无机电极材料价格昂贵及含有毒金属的问题, 也不存在有机小分子循环稳定性差的问题, 在下一代可充电金属离子电池中具有巨大的应用潜力。因此, 本文总结了共价有机框架电极材料的电化活性位点, 并着重讨论了通过调节共价有机框架的骨架结构、孔道、活性位点和电子结构提高共价有机框架电极材料电化性能(包括: 能量密度、倍率性能和循环寿命)的策略。为了开发高性能的共价有机框架电极材料, 未来的工作需着重于优化它们的离子和电子导电性, 进一步提高它们的工作电压以及探明它们的储能机制。本文将有助于开发用于下一代金属离子电池的高性能共价有机框架电极材料。

**关键词:** 共价有机框架; 可充电金属离子电池; 能量密度; 倍率性能; 循环寿命

**文章编号:** 1007-8827(2021)01-0001-18

**中图分类号:** TQ127.1<sup>+1</sup>

**文献标识码:** A

**基金项目:** 国家自然科学基金(51425302, 51302045); 北京市自然科学基金(2182086).

**通讯作者:** 马英杰, 助理研究员. E-mail: mayj@nanoctr.cn;

智林杰, 教授, 博士生导师. E-mail: zhilj@nanoctr.cn

**作者简介:** †曾术茂, 黄小雄为共同第一作者

本文的电子版全文由 Elsevier 出版社在 ScienceDirect 上出版 (<http://www.sciencedirect.com/science/journal/18725805>)